Effects of Various Small-Molecule Anesthetics on Vesicle Fusion: A Study Using Two-Photon Fluorescence Cross-Correlation Spectroscopy

Trinh T. Nguyen, Jody L. Swift, Melanie C. Burger, and David T. Cramb*

Department of Chemistry, University of Calgary, 2500 University Drive N.W., Calgary, Alberta T2N 1N4, Canada

Received: February 5, 2009; Revised Manuscript Received: June 5, 2009

Currently, the molecular mechanism for membrane fusion remains unconfirmed. The most compelling suggested mechanism is the stalk hypothesis, which states that membrane fusion proceeds via stalk formation/hemifusion, among other steps. Because the stalk would have a very high radius of curvature, small lipophilic molecules could enhance fusion by lowering the energy barrier to stalk formation. We previously showed that the general anesthetic halothane is capable of inducing membrane fusion in 1,2-dileoyl-*sn*-3-glycero-3-phospocholine (DOPC) vesicles. In the present study, we examined other small molecules, general anesthetics (chloroform, isoflurane, enflurane, and sevoflurane), to determine whether they exhibit fusion properties with model lipid membranes similar to those of halothane. We employed both two-photon excitation fluorescence cross-correlation spectroscopy (TPE-FCCS) and steady-state fluorescence dequenching (FD) assays. Using volatile general anesthetics as novel fusion agents, we also aimed to gain a better understanding of the membrane fusion mechanism at a molecular level. We found that lipid mixing or lipid rearrangement, which is required for the formation of the fusion-state intermediates and the fusion pore, rather than the association of lipid vesicles, is rate-limiting. In addition, halothane and chloroform were found to induce lipid mixing (rearrangement) to a greater extent than isoflurane, enflurane, and sevoflurane. Finally, it is proposed that the efficiency of these general anesthetics as fusion agents is related to their partition coefficients, water solubilities, polarities, and molecular volumes, all of which affect the ability of each anesthetic to perturb the contacting bilayer membranes of fusing vesicles.

Introduction

Membrane fusion is the process in which two phospholipid bilayers merge together in an aqueous environment to form a single mixed lipid bilayer.[1] Fusion is an essential mechanism in the function of eukaryotic cells and is involved in the transport of food and waste, intercellular communication, sexual reproduction, and the asexual transfer of genetic material.[2] Moreover, membrane fusion is believed to be the crucial event in the origin of life, which has attracted the interest of researchers to develop a model explaining the fusion process.[1] Although the exact mechanism of membrane fusion has been under debate for many years, it is now generally accepted that both proteins and lipids play important roles in the process of fusion, as the rearrangement of lipid structures is an essential step in the fusion mechanism.[3] The current supported mechanism for membrane fusion includes the following stages: aggregation/contact, stalk formation/hemifusion, trans-monolayer contact, and finally the formation of a fusion pore, which is followed by the complete mixing of the vesicle contents (Figure 1A[4]).[5] Figure 1A shows that a bilayer will have both positive and negative curvature during stalk formation and that these highly curved states can act as barriers to fusion.

Considerable recent work has helped to elucidate important steps in vesicle fusion. Cummings and Vanderlick[6] have illustrated that vesicle aggregation kinetics can be described as a two-step process: step one involves vesicle−vesicle collision, whereas step two involves the union of the membrane. It was deduced for the crypdin-4 peptide-mediated aggregation of lipid vesicles that the union of the membrane is rate-limiting.[6] Additionally, studies examining the kinetics of the lipid mixing in membrane fusion have indicated the presence of kinetically long-lived intermediates that progress to a hemifusion state, which is followed by a rate-determining step toward the formation of a fusion pore.[7] Almost all of the previous vesicle fusion kinetics studies have employed lipid bilayers that contain proteins.

In contrast, we chose to examine vesicles made from a single type of lipid, 1,2-dileoyl-*sn*-3-glycero-3-phospocholine (DOPC), which could provide insight into the lipid bilayer properties that effect fusion. Our recent work in this area has shown that the presence of halothane ($CF_3CHClBr$), an anesthetic that is regularly used in veterinary medicine and in drug−protein binding studies,[8] can induce changes in the electrostatic interactions within the bilayer, which results in thinning of supported bilayers.[9,10] Halothane was also found to be capable of quenching gramicidin D fluorescence, with the maximum interaction between halothane and gramicidin D occurring within the lipid bilayer.[8]

In addition, we have previously demonstrated that fluorescence correlation spectroscopy (FCS) can be used to examine steps in lipid vesicle fusion.[11] FCS is a powerful tool that is widely used for the dynamic characterization of biomolecules in vitro. Two-photon excitation fluorescence cross-correlation spectroscopy (TPE-FCCS) is capable of measuring the association and dissociation of two species labeled with different fluorescent labels over time within a defined focal volume. Concentrations of bound and individual unbound labeled species can be determined from the amplitude of the cross- and autocorrelation analyses respectively. The diffusion coefficients of these species can also be extracted from the correlation decay,

* Corresponding author. E-mail: dcramb@ucalgary.ca.

10.1021/jp901089k CCC: $40.75
Published on Web 07/06/2009

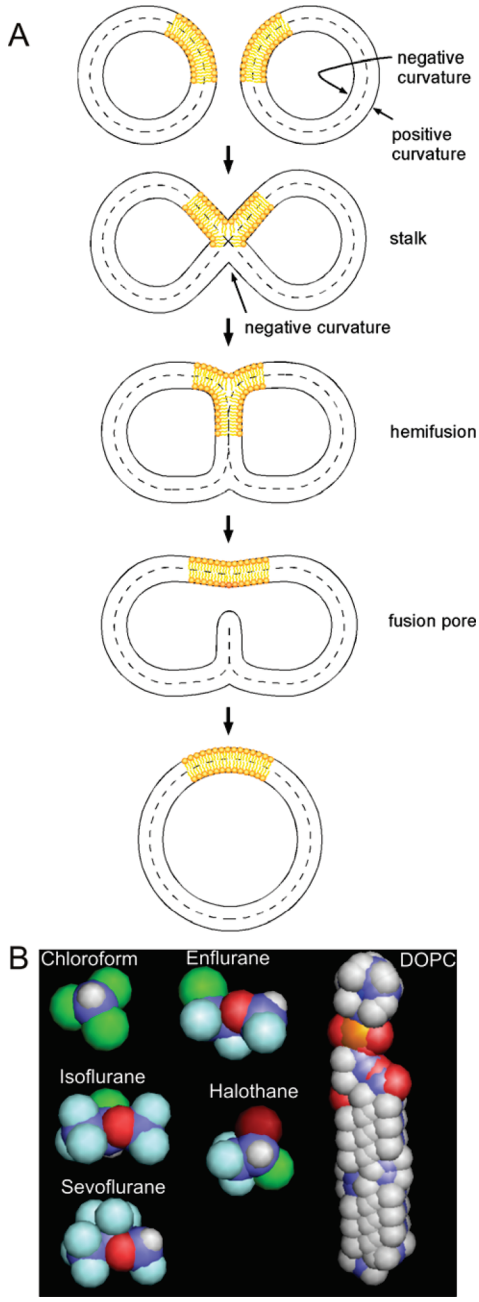

Figure 1. (A) Illustration of the mechanism of vesicle fusion.[4] Outer membrane contact results in lipid mixing of the outer membrane leaflet, which produces the fusion stalk and hemifusion state. The subsequent steps included trans-monolayer contact and subsequent lipid mixing in the formation of the fusion pore and complete membrane fusion. Reproduced with permission from ref 4. (B) Space-filling structures of the phospholipid and anesthetics used in this study. The space-filling molecular models were drawn using PyMol (DeLano Scientfic, San Carlos, CA).

and therefore their respective hydrodynamic radii can be determined using the Stokes−Einstein relationship.[12,13]

Previously, we demonstrated halothane's ability to enhance membrane fusion in model DOPC vesicles in the absence of membrane proteins,[11] which supports the idea that lipids play an essential role in the mechanism of membrane fusion. In the present study, we investigated whether other small lipophilic molecules, namely, the general anesthetics chloroform, isoflurane, enflurane, and sevoflurane (Figure 1B), shared similar fusion-/hemifusion-enhancing properties on DOPC vesicles. With this type of study we aim to understand the interactions between general anesthetics and lipid membranes and gain a better knowledge of the mechanism which explains anesthetic induced membrane fusion.

It is predicted that enhanced membrane fusion/hemifusion in the presence of anesthetics is dependent on where the anesthetic incorporates into the bilayer and on the lipophilicity of the anesthetic. The general anesthetic halothane was previously shown to localize in the bilayer just below the headgroup region.[14] Baber et al.[15] also showed that halothane, enflurane, and isoflurane localize evenly in the hydrocarbon region of the bilayer near the membrane−solution interface.[15] The presence of these general anesthetics below the headgroup of the bilayer perturbs the membrane. This perturbation can lead to a lateral swelling perpendicular to the bilayer plane[16] and can also increase the occurrence of lipid rearrangement, resulting in a greater potential for the formation of fusion intermediates that can progress into fusion pore states.[11,15,17] Moreover, if other general anesthetics incorporate into the bilayer in a manner similar to halothane,[15] we would expect to observe similar fusogenic properties. Finally, one might expect that the potency of these general anesthetics as fusion agents is related to their partition coefficients, polarities, and molecular volumes.

Materials and Methods

1,2-Dileoyl-*sn*-3-glycero-3-phospocholine (DOPC) and lissamine [red label; 1,2-dioleoyl-*sn*-glycero-3-phosphoethanolamine-*N*-(lissamine rhodamine B sulfonyl) (ammonium salt)] were obtained from Avanti Lipids. β-BODIPY-C5-HPC (530/550) [2-(4,4-difluoro-5,7-diphenyl-4-bora-3a,4a-diaza-*s*-indacene-3-pentanoyl)-1-hexadecanoyl-*sn*-glycero-3-phosphocholine, which from now on will be referred to as BODIPY] and Oregon Green (green label; Oregon Green 488 1, 2-dihexadecanoyl-*sn*-glycero-3-phosphoethanolamine) were obtained from Invitrogen. 1-Bromo-1-chloro-2,2,2-trifluoroethane (halothane), 2-chloro-1,1,2-trifluoroethyl difluoromethyl ether (enflurane), 1-chloro-2,2,2-trifluoroethyl difluoromethyl ether (isoflurane), and 1,2,2,2-tetrafluoroethyl difluoromethyl ether (sevoflurane) were purchased from Alfa Aesar. Spectroscopic-grade chloroform was purchased from Sigma. All lipids, fluorescent labels, and anesthetics were not purified further prior to use. Stock solutions of DOPC ($\sim 3.5 \times 10^{-3}$ M), BODIPY (1.08×10^{-5} M), Oregon Green (9.21×10^{-5} M), and lissamine (7.86×10^{-5} M) were prepared in chloroform and were stored at −20 °C until use. Quartz sample chambers were used throughout all experiments.

Fluorescence Dequenching (FD) Assay.[18] Appropriate amounts of DOPC and BODIPY stock solutions were used to yield DOPC and BODIPY concentrations of 0.1 mM and 5 μM, respectively. N_2 gas was used to evaporate all the solvent, and the dried labeled lipid was resuspended in a phosphate-buffered saline (PBS) buffer containing 320 mM sucrose.[11] Unlabeled DOPC vesicles were produced similarly. To produce large unilamellar vesicles (LUVs), both labeled and unlabeled samples were stirred in the dark for 30 min at room temperature to allow for the complete resuspension of the lipid into the buffer. After adequate mixing, the samples were alternately sonicated and stirred until they became clear (approximately five cycles), after which they were stored in the dark at 4 °C for no more than 7 days. Prior to experimentation, samples were extruded[19] using an Avanti Polar Lipids Inc. miniextruder equipped with a 100-nm nuclepore track-etch membrane purchased from Whatman Nuclepore.

A 5:1 (v/v) ratio of unlabeled to labeled DOPC LUVs was pipetted into a 10-mm-path-length fluorescence cuvette. The

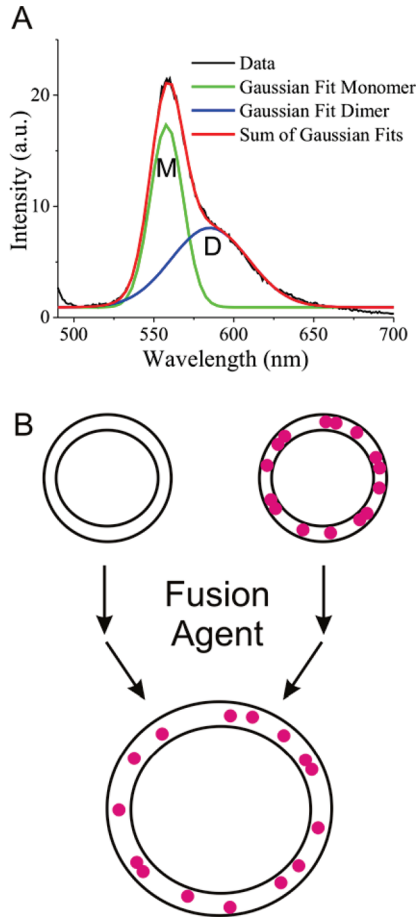

Figure 2. Fluorescence emission spectrum for DOPC (0.1 mM, lipid) vesicles labeled with β-BODIPY-C5-HPC (5 μM) excited at 480 nm. (A) Emission spectrum containing contributions from BODIPY monomers and dimers, which are modeled by Gaussian peaks (green and blue curves, respectively). The sum of the Gaussian peaks produces the fit (red curve) to the raw data (black curve). (B) Schematic of the fusion of an unlabeled vesicle and a labeled vesicle in the presence of a fusion agent (anesthetic). The fusion of the two vesicles separates some of the BODIPY dimer molecules into monomers.

sample was then inverted several times to ensure complete mixing, and an emission spectrum was obtained. An anesthetic [halothane, chloroform, enflurane, isoflurane, or sevoflurane (2% v/v)] was added to the cuvette, and the sample was inverted 10 times to ensure rapid mixing.[9,14] In the case of chloroform, this produced a saturated solution (~70 mM). Fluorescence experiments were conducted using a Varian Cary Eclipse fluorescence spectrometer. The instrument was set to a medium scan speed, and both emission and excitation slit widths were set to 5 nm. Emission spectra were obtained by exciting the sample at 480 nm and collecting the emission from 490 to 700 nm. Spectra were obtained every 5 min after anesthetic addition for 15 min, then every 15 min for 90 min, and finally every 30 min thereafter until a total of 360 min had elapsed.[11] We also measured the maximum extent of dequenching by collecting fluorescence data from a solution with the BODIPY label dispersed evenly among all of the vesicles in an effective dilution by 5. This allowed for a direct comparison with the above data.

All spectra that were collected were plotted and fitted using Origin Pro 7.0. To determine the BODIPY fluorescence dequenching (FD) contributions from the dimer and monomer peaks, the data were fit using the sum of two Gaussian functions,[11] as illustrated in Figure 2. The dimer peak center was held fixed at 16979 cm^{-1}, the monomer peak center was held fixed at 17952 cm^{-1}, and the ratio of the peak areas was determined for each spectrum.

Data Reduction. Previous work that utilized the BODIPY FD assay[11] examined fluorescence data by plotting the ratio of integrated fluorescence of monomer to dimer ($A_{monomer}/A_{dimer}$) as a function of time. The shape of the plot was then compared to normalized TPE-FCCS data to confirm the occurrence of fusion/hemifusion. However, rate constants of fusion/hemifusion obtained by the two methods could not be directly compared with each other. Therefore, the proposed fusion/hemifusion mechanism of the BODIPY dequenching assay was further investigated to produce rate constants that were directly comparable to those obtained by TPE-FCCS. Assuming that the fusion/hemifusion of an unlabeled vesicle with a labeled vesicle is the only fusion/hemifusion event that is occurring early in the reaction, the following equation can be used to represent fusion/hemifusion kinetics in the FD assay

$$DOPC_{(D)} + DOPC \rightarrow DOPC_{2(M)} \quad (1)$$

where $DOPC_{(D)}$ represents a labeled DOPC vesicle containing BODIPY dimers that fuses with an unlabeled DOPC vesicle to produce a larger DOPC vesicle ($DOPC_{2(M)}$) that contains BODIPY monomers and some dimers. The increase in monomer intensity (equivalent to the monomer concentration) can be represented by the differential rate law

$$\frac{d[DOPC_{2(M)}]}{dt} = k[DOPC_{(D)}][DOPC] \quad (2)$$

The reaction can also be described with respect to the change in dimer concentration using the equation

$$\frac{d[DOPC_{(D)}]}{dt} = -k[DOPC_{(D)}][DOPC] \quad (3)$$

If the concentration of unlabeled vesicles is in excess, eq 3 can be reduced to the pseudo-first-order rate law

$$\frac{d[[DOPC_{(D)}]}{dt} = k'[DOPC_{(D)}] \quad (4)$$

The integrated rate law of eq 4 is

$$[DOPC_{(D)}] = [DOPC_{(D)}]_0 e^{-k't} \quad (5)$$

The increase in the concentration of $DOPC_{2(M)}$ due to the loss of dimer can be represented by the equation

$$[DOPC_{2(M)}] = [DOPC_{(D)}]_0 - [DOPC_{(D)}] \quad (6)$$

Substitution of eq 5 into eq 6 yields

$$[DOPC_{2(M)}] = [DOPC_{(D)}]_0 - [DOPC_{(D)}]_0 e^{-k't} \quad (7)$$

However, we must consider and account for the initial presence of monomer, as the initial labeled vesicle will contain not only BODIPY dimers, but some monomer as well. Therefore

$$[\mathrm{DOPC}_{2(\mathrm{M})}] = [\mathrm{DOPC}_{2(\mathrm{M})}]_0 + ([\mathrm{DOPC}_{(\mathrm{D})}]_0 - [\mathrm{DOPC}_{(\mathrm{D})}]_0 e^{-k't}) \quad (8)$$

Equation 8 can then be rearranged and simplified to yield

$$\frac{[\mathrm{DOPC}_{2(\mathrm{M})}] - [\mathrm{DOPC}_{2(\mathrm{M})}]_0}{[\mathrm{DOPC}_{(\mathrm{D})}]_0} = 1 - e^{-k't} \quad (9)$$

where the concentrations of $\mathrm{DOPC}_{2(\mathrm{M})}$ and $\mathrm{DOPC}_{(\mathrm{D})}$ are represented by the corresponding areas under the BODIPY emission peak intensities.

TPE-FCCS Measurements. Appropriate amounts of lissamine and Oregon Green lipid labels were added to DOPC to produce concentrations of 400 and 250 nM, respectively. A larger concentration of lissamine was required because of a greater loss during extrusion.[11] Labeled vesicles were produced in PBS, using the previously outlined procedure.[11] Prior to experimentation, the respectively labeled samples were extruded, and 500 μL of each was pipetted into an Eppendorf tube. Then, 2% (v/v) anesthetic was added, and the sample was inverted 10 times to ensure complete mixing. Next, 400 μL of the sample was placed into a quartz sample chamber and was immediately placed on the inverted microscope. Fluorescence autocorrelation and cross-correlation decays were collected every 5 min for the first 15 min after anesthetic addition, then every 15 min for 90 min, and finally every 30 min thereafter until a total of 360 min had elapsed.

Samples were excited at 780 nm, by a 100-fs pulsed Spectra Physics Tsunami Ti:sapphire laser operated at 82 MHz. The laser power was set to 30 mW with a neutral density filter. In-depth instrumental information and parameters were provided previously by Swift et al.[11]

Data Reduction. Assuming a Gaussian two-photon excitation (TPE) volume, autocorrelation decay curves were modeled and fitted using the equation[20]

$$G(\tau) = G(0)\left(1 + \frac{8D\tau}{r_0^2}\right)^{-1}\left(1 + \frac{8D\tau}{z_0^2}\right)^{-1/2} \quad (10)$$

where D is the diffusion coefficient, τ is the lag time, $G(0)$ is the correlation amplitude, r_0 is the radius of the laser beam, and z_0 is the depth of the focal volume. The size of the volume of excitation was calibrated using 5.9 nM, 40 nm FluoSpheres (Invitrogen) and was determined to be 3.4 ± 0.8 fL.

Cross-correlation decays were modeled and fitted using the equation[20]

$$G_{ij}(\tau) = G_x(0)\left(1 + \frac{8D\tau}{r_0^2}\right)^{-1}\left(1 + \frac{8D\tau}{z_0^2}\right)^{-1/2} \quad (11)$$

where the subscripts i, j, and ij are for red-labeled, green-labeled, and dual-color-labeled diffusing species, respectively, and $G_x(0)$ is the cross-correlation amplitude.

Complete separation between the two detection channels of Oregon Green and lissamine emissions is not possible, as some of the Oregon Green emission will be detected the lissamine (red) channel. To account for this unspecific crosstalk, the particle brightness for each fluorophore in each detection channel must be considered.[12] Therefore, the concentration of the dual-color-labeled species, C_{ij}, can be defined by the equation[12]

$$C_{ij}(t) = \frac{8\langle F_i\rangle\langle F_j\rangle G_x(0,t)}{\eta_{ii}\eta_{jj}V_{\mathrm{eff}}} - \frac{C_{i,0}\eta_{ij}}{\eta_{jj}} \quad (12)$$

where F_i and F_j are the average fluorescence intensities from the green and red detection channels, respectively, in counts per second. $G_x(0,t)$ represents the individual amplitudes of the cross-correlation decay curve at a given time t. η_{ii} is the apparent brightness of the green fluorophore, η_{jj} is the apparent brightness of the red fluorophore, and η_{ij} is the crosstalk of the green fluorophore in the red detection channel, all expressed in counts per molecule per second.

The chemical equation used to represent the fusion/hemifusion kinetics of the association of an equimolar distribution of vesicles labeled with red and green dyes in the TPE-FCCS assay is

$$4\mathrm{R} + 4\mathrm{G} \rightarrow 2\mathrm{RG} + \mathrm{RR} + \mathrm{GG} \quad (13)$$

where R and G represent red- and green-labeled vesicles, respectively, and RG represents the fused/hemifused red and green vesicles. RR is the result of the fusion/hemifusion of two red-labeled vesicles, and GG is the result of the fusion/hemifusion of two green-labeled vesicles. Thus, in the TPE-FCCS fusion/hemifusion assay, one has a mixture of fused/hemifused species, some with twice the brightness of the original and some with the same brightness.

Equation 12 accounts for crosstalk of green fluorescence in the red detection channel. However, eq 12 does not distinguish that some of the fused/hemifused species will have twice the brightness, when same-colored vesicles fuse together. Subsequently, their brightness will factor into the interpretation of the $G(0)$ values for both the auto- and cross-correlation decays. Therefore, for the cross-correlation decays, the follow relationship was established

$$G_{ij}(0) = \frac{\sum_k \eta_{kii}\eta_{kjj}N_{\mathrm{RG}}}{\sum_k \eta_{kii}N_{k\mathrm{G}}\sum_k \eta_{kjj}N_{k\mathrm{R}}} = \frac{\eta_{ii}\eta_{jj}N_{\mathrm{RG}}}{[\eta_{ii}(N_{\mathrm{R}} + N_{\mathrm{RG}}) + 2\eta_{ii}N_{2\mathrm{R}}][\eta_{jj}(N_{2\mathrm{R}} + N_{\mathrm{RG}}) + 2\eta_{jj}N_{2\mathrm{R}}]} \quad (14)$$

where N_{RG} is the number of red−green fused/hemifused species, N_{R} is the number of monomer red species, N_{G} is the number of monomer green species, and $N_{2\mathrm{R}}$ is the number of red−red fused/hemifused species. Assuming that the brightness does not change as a function of binding, the absolute particle brightnesses for the two fluorescent species (η_{ii} and η_{jj}) cancel out in eq 14. Moreover, when $N_{\mathrm{G}} = N_{\mathrm{R}}$, we can further simplify eq 14 to obtain

$$G_{ij}(0) = \frac{N_{\mathrm{RG}}}{(N_{\mathrm{R}} + N_{\mathrm{RG}} + 2N_{2\mathrm{R}})^2} \quad (15)$$

Note that $N_{\mathrm{R,total}} = N_{\mathrm{R}} + N_{\mathrm{RG}} + 2N_{2\mathrm{R}} = N_{\mathrm{R}}(\mathrm{initial})$, which applies only in the case of the fusion/hemifusion of monomers to form dimers

$$G_{ij}(0) = \frac{N_{\mathrm{RG}}}{[N_{\mathrm{R}}(\mathrm{initial})]^2} \quad (16)$$

Therefore, theoretically, the cross-correlation amplitude should start at zero and increase to a value of $1/(2N_R)^2$ for the formation of dimers. Our data show that the cross-correlation amplitude does not start at zero, because some green fluorescence leaks into the red channel, which results in a low apparent cross-correlation that is not real.

We can examine the autocorrelation decays in a similar fashion, using the same assumptions as previously applied in the analysis of the cross-correlations decays, which results in the following equation for the red channel

$$G(0) = \frac{\sum_k \eta_k^2 N_k}{(\sum_k \eta_k N_k)^2} = \frac{\eta_{jj}^2(N_R + N_{RG}) + 4\eta_{jj}^2 N_{2R}}{[\eta_{jj}(N_R + N_{RG}) + 2\eta_{jj}N_{2R}]^2} = \frac{N_R + N_{RG} + 4N_{2R}}{[N_R(\text{initial})]^2} \quad (17)$$

Simplifying eq 17 yields

$$G(0) = \frac{1}{N_R(\text{initial})} + \frac{2N_{2R}}{[N_R(\text{initial})]^2} = \frac{1}{N_R(\text{initial})} + \frac{1}{2N_R(\text{initial})} = \frac{3}{2}\frac{1}{N_R(\text{initial})} \quad (18)$$

Equation 17 can be applied similarly to the green channel, substituting the corresponding number of particles and particle brightness for the green fluorophore. Thus, as red or green monomers fuse together to form dimers, the amplitudes of the autocorrelation functions in the two channels will remain constant. However, at longer time scales, higher-order fusion/hemifusion events might occur, which could cause a slight increase in the autocorrelation amplitudes to be observed. All fitting of the data was performed using Origin Pro 7.0.

Results

Lipid Mixing: Fluorescence Dequenching Fusion/Hemifusion Assay. The fluorescence dequenching (FD) assay was derived from a fluorescence resonance energy transfer (FRET) fusion/hemifusion assay that utilized the FRET donor−acceptor pair of BODIPY 500-PC and BODIPY 530-PE.[18] In the previously published FRET assay, lipid vesicles containing both FRET donors and acceptors were fused with unlabeled lipid vesicles containing no fluorescent probes. The resultant dilution of the donor−acceptor pairs would lead to an increase in the distances between the FRET donor−acceptor pairs, thus reducing the intensity of the FRET signal.

BODIPY is known to dimerize at high concentrations (0.5−2.5 mol %), and therefore, it can be used in an FD fusion/hemifusion assay similar to previously used FRET assays.[11] Indeed, we have previously demonstrated that the fluorescence dequenching assay is a valid reporter on lipid mixing, by comparing FD results with those from contents mixing.[11] Figure 2A shows a fluorescence emission spectrum composed of monomer and dimer emissions from BODIPY 530/550 incorporated into DOPC vesicles. The blue and green peaks represent the Gaussian deconvolutions corresponding to the BODIPY dimer and monomer, respectively, which emit at slightly different wavelengths. Because of the spectral overlap between the two, the excimer (dimer) peak appears to increase, but this is not actually the case. The red plot in Figure 2A is the fit obtained from the sum of the blue and green Gaussian peaks, whereas the black plot is the experimental data. Figure 2B shows a schematic of the FD assay, which involves the fusion/hemifusion a nonfluorescently labeled lipid vesicle with a vesicle that contains a high concentration of the BODIPY probe. This process can be interpreted in the following way (as illustrated in Figure 1[4]): As membrane hemifusion proceeds, lipid mixing of the contacting (proximal) monolayers of the vesicles occurs as part of the initial stalk formation. Eventually, the stalk expands, and mixing of the inner (distal) lipid monolayers results. The lipid rearrangement required to produce the fusion stalk and fusion pore can be monitored using the FD assay, as fusion/hemifusion of the unlabeled vesicles results in a dilution of BODIPY dimers within the labeled vesicles. The increase in lipid concentration separates the BODIPY dimers into monomers, and an increase in monomer intensity can be observed.

Emission spectra from a mixture of labeled and unlabeled vesicles were collected over time in the presence of either chloroform or sevoflurane. Examples are presented in Figure 3A,B. It is clear that the monomer peak intensity increases with time in both cases; however, the effect is much more pronounced

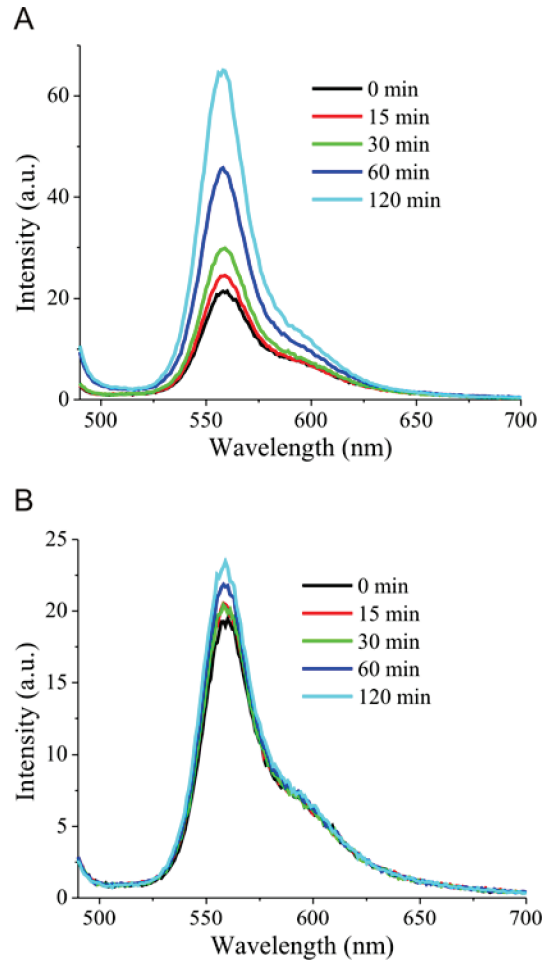

Figure 3. (A) Fluorescence spectra of BODIPY (5 μM) labeled DOPC (0.1 mM, lipid) vesicles mixed with unlabeled vesicles as a function of time after chloroform (2% v/v) addition. There is an increase in monomer fluorescence as fusion occurs between labeled and unlabeled vesicles. (B) Fluorescence spectra of BODIPY (5 μM) labeled DOPC (0.1 mM, lipid) vesicles mixed with unlabeled vesicles as a function of time after sevoflurane (2% v/v) addition. All samples were excited at 480 nm, and spectra were collected over time using a Varian Cary Eclipse fluorescence spectrometer.

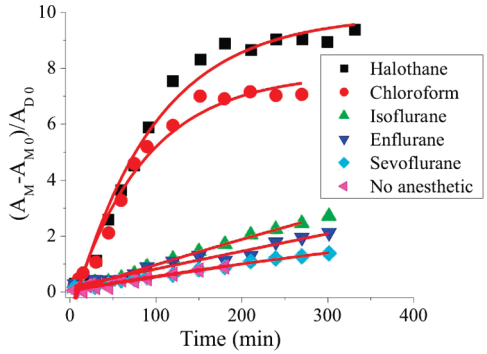

Figure 4. Kinetic curves for the fusion of BODIPY (5 μM) labeled and unlabeled DOPC (0.1 mM, lipid) vesicles induced by various anesthetics (2% v/v). Vesicle samples were excited at 480 nm, the resultant fluorescence spectra were collected, and emission contributions from the BODIPY monomer and dimer were deconvoluted as shown in Figure 2. A ratio of emission peak areas was plotted as a function of time, and these curves were fit with eq 9; the results of the fits are summarized in Table 1.

in the case where chloroform was used as the fusion agent. Over the span of 120 min, the monomer peak intensity increased 225% in the case of chloroform, compared to sevoflurane, whose monomer peak intensity increased only by 21%. The percent increases of monomer intensity for the remaining anesthetics were 227%, 37%, and 33% for halothane, isoflurane, and enflurane, respectively.

By plotting the ratios of the monomer and dimer peak contributions, according to eq 9, one can compare the effectiveness of each anesthetic as a fusion/hemifusion-inducing agent, as illustrated in Figure 4. The data shown in Figure 4 can be separated into two distinct categories: anesthetics that induced the greatest amount of lipid mixing (halothane and chloroform), evidenced by the largest increases in monomer fluorescence intensity, and anesthetics that induced little or no lipid mixing (isoflurane, enflurane, and sevoflurane), resulting in smaller changes in monomer fluorescence intensity. Assuming that the unlabeled vesicles were in excess, the data for each anesthetic in Figure 4 were fit using eq 9 (red curve), and corresponding rate constants for the lipid mixing stage of the fusion mechanism were obtained. Note that these are the true rate constants, k, as k' values determined from the fits were divided by the initial unlabeled vesicle concentration, consistent with eqs 3 and 4. The rate constants of lipid mixing for the various anesthetics were similar within the experimental error for chloroform, halothane, and isoflurane and were found to be greater than the rate constants for both enflurane and sevoflurane (Table 1).

It is possible that anesthetics induce bilayer swelling. This swelling could effectively dilute the fluorescent labels, thus altering the monomer/dimer peak ratios. To determine whether there was any contribution from bilayer swelling to the increase in monomer intensity, the FD assay was conducted in the absence of the unlabeled DOPC vesicles. Assuming the concentration of the fluorescent probe to be the same in each vesicle, one would expect no change in monomer fluorescence intensity to be observed upon addition of anesthetic, unless some swelling of the bilayer occurred. The results from the fusion/hemifusion of fluorescently labeled and unlabeled DOPC vesicles (squares) and from fusion/hemifusion in the absence of unlabeled vesicles (circles) for the anesthetics halothane, chloroform, and isoflurane (black, green, and red, respectively) are summarized in Figure 5. Upon comparison of the results, it is clear that the increase in monomer fluorescence intensity is vastly reduced in the absence of unlabeled lipid vesicles.

It is also possible that an aqueous solution saturated with chloroform would promote significant lipid exchange without fusion, or even possible dissolution of the vesicles. Similarly, nanoclusters of alcohols in water have been suggested by molecular dynamics simulations.[21,22] Therefore, further experiments were performed to determine whether this was the case. The results are presented in the Supporting Information and summarized here. We found no evidence of fluorescent label transfer between vesicles via the chloroform-saturated aqueous solution. In contrast, we found evidence of vesicles decreasing in number and increasing in size and brightness in the chloroform-saturated solution. This is an indication of association, rather than dissolution.

Early Stages in Vesicle Fusion: FCCS Assay. Although the above fluorescence dequenching assay is simple, it does not distinguish lipid mixing events from vesicle−vesicle association. We therefore chose to apply an assay that reports on vesicle association rates. As described previously by Swift et al.,[11] FCCS amplitudes can be used to determine the concentration of associated vesicles versus time after addition of a fusion-enhancing agent. An example of the cross-correlation data from the present study is shown in Figure 6, which shows "before" and "after" anesthetic count-rate trajectories (Figure 6A,B); a typical FCCS decay, with fit to eq 11 (Figure 6C); and a pictorial representation of the vesicle association process (Figure 6D). The amplitude of the cross-correlation decay curve is proportional to the number of the associated/bound red−green species within the TPE volume, and the resultant concentration of associated/bound species can be plotted as a function of time after anesthetic addition (Figure 7). Assuming that the association and fusion/hemifusion of vesicles can be described as a simple binary reaction, the fusion/hemifusion kinetics can be modeled with a second-order integrated rate law using eqs 16 and 17. Fluorescence resonance energy transfer (FRET) between the red and green labels in associated vesicles would complicate the FCCS analysis. However, we see no evidence of FRET taking place. This conclusion can be gleaned from the count-rate trajectories in Figure 6A,B, where the fluorescence level does not change after the addition of anesthetic. If FRET were occurring, one would expect a decrease in the green channel and an increase in the red channel.

The average association plots for each anesthetic (three trials, averaged) are shown in Figure 7A. It can be seen that, within the experimental error, the data for all of the anesthetics are quite similar, as the maximum concentration of associated red−green vesicles for all anesthetics ranges between approximately 1×10^{-10} and 2×10^{-10} M. The second-order kinetic data in Figure 7A were linearized by plotting the inverse concentration of associated red and green vesicles as a function of time, as shown in Figure 7B. The slope of the linearized data yields the rate constant for the association of red and green vesicles with each other. At long experiment times, higher-order fusion/hemifusion events are probable, and the resultant data become difficult to interpret. Therefore, short time scales (less than 30 min) were examined. The rate constants obtained from the slopes of the linearized second-order data for chloroform, halothane, isoflurane, enflurane, and sevoflurane are summarized in Table 1.

Finally, we can support the assumptions made in our derivation of the association kinetics of red and green fluorescently labeled vesicles, which resulted in eqs 17 and 18, by plotting the amplitudes of the autocorrelation functions ($G_{(0)}$) for both the red and green detection channels as functions of time (Figure 8). It is clear from Figure 8 that the amplitudes of

TABLE 1: Summary of Rate Constants Obtained from Steady-State Fluorescence Dequenching (FD) Lipid Mixing and Two-Photon Excitation Cross-Correlation Spectroscopy (TPE-FCCS) Association Assays, Molecular Dipoles, and Molar Volumes, and Oil/Water Partition Coefficients (P_{ow}) for the General Anesthetics Halothane, Chloroform, Isoflurane, Enflurane, and Sevoflurane

anesthetic	FD lipid mixing rate constant (M^{-1} min^{-1})	FCCS association rate constant (M^{-1} min^{-1})	extent of lipid mixing (%)	μ (D)	molar volume (Å^3)	P_{ow}
halothane	$2.10 (\pm 0.35) \times 10^4$	$5.79 (\pm 2.12) \times 10^7$	59	1.5[37,38]	66	313
chloroform	$2.62 (\pm 0.70) \times 10^4$	$2.18 (\pm 0.89) \times 10^8$	51	1.0[39]	80[40]	61
isoflurane	$1.92 (\pm 0.18) \times 10^4$	$1.72 (\pm 0.68) \times 10^9$	21	2.0[41]	127[40]	168
enflurane	$1.22 (\pm 0.18) \times 10^4$	$2.53 (\pm 0.77) \times 10^8$	15	0.7[41]	122[40]	124
sevoflurane	$1.05 (\pm 0.03) \times 10^4$	$9.57 (\pm 3.86) \times 10^7$	11	2.3[37]	133[40]	148

the autocorrelation functions for both the red and green detection channels remain relatively constant for the duration of the experiment. The slow progressive increases in the $G_{(0)}$ values at longer times suggest higher-order (i.e., more than two vesicles) association events.[6]

Discussion

Recent work by Weinreb and Lentz[17] demonstrated the complexity of the vesicle fusion process. They proposed a model in which a rapid association step is followed by rate-limiting stalk-formation steps. Further, they detailed the possibility of fusion occurring through two sequential intermediate states and suggested that, within these states, lipid mixing, contents mixing, and contents leakage can all occur simultaneously.[17] Our work aimed to probe two different stages in the fusion mechanism: the initial aggregation or contact of vesicles and the process of lipid mixing toward complete vesicle fusion.

Upon comparison of the rate constants in Table 1, the general trend of association being faster than lipid mixing is clear. We conclude that this behavior arises as follows: FCCS reports on the initial association steps, because only associated vesicles register a cross-correlation signal. This can be compared with the fluorescence dequenching assay, which reports only on changes in the fluorescent-lipid concentration and therefore is not sensitive to association without lipid mixing. The average rate constant for lipid mixing is 4 orders of magnitude lower than that for association. Interestingly, anesthetics increase both the association and lipid mixing rates, but apparently not in the same way.

Lipid Mixing and Anesthetics. Lipid mixing can be associated with hemifusion and/or full fusion.[17] The extent (i.e., maximum amount) of lipid mixing, as shown in Figure 4 and summarized in Table 1, follows the trend halothane > chloroform > isoflurane > enflurane > sevoflurane. In contrast, the trend observed for the lipid mixing rate constants was chloroform ≈ halothane ≈ isoflurane > enflurane ≈ sevoflurane. When comparing the extent of lipid mixing due to each anesthetic with the rate constant for lipid mixing, the trends observed are quite similar. The differences observed in the extent and rate constants of lipid mixing for each of the anesthetics should be due to their molecular properties. One might expect that the anesthetic position and/or quantity in the bilayer would be important in this respect. Therefore, trends of lipid mixing as a function of bilayer partitioning, molecular volume, and electric dipole moment were examined.

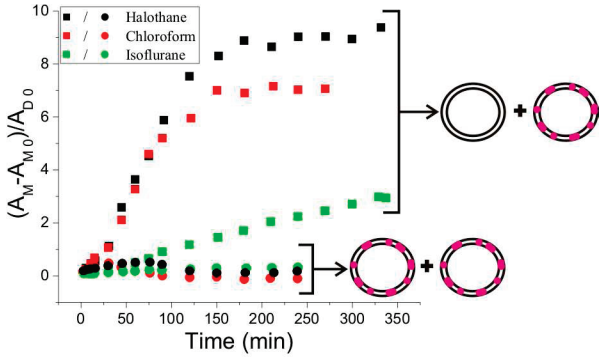

Figure 5. Comparison of normalized kinetic curves for the fusion of BODIPY (5 μM) labeled and unlabeled DOPC (0.1 mM, lipid) vesicles induced by 2% v/v anesthetic concentration of halothane (black squares), chloroform (red squares), and isoflurane (green squares), previously shown in Figure 4, to respective controls that contained no unlabeled vesicles (black, red, and green circles).

Oil/water partition coefficients were determined by taking the ratio[23] of known oil/gas and water/gas partition coefficients.[24,25] Table 2 summarizes the known octanol/water partition coefficients, calculated oil/water partition coefficients, and water solubilities for all of the anesthetics used. It is notable that an increasing partition coefficient is correlated with increases in the extent of lipid mixing and the lipid mixing rate constant. An exception to this trend is chloroform, which has the lowest partition coefficient, highest lipid mixing rate constant, and the second largest extent of lipid mixing. The discrepancy for chloroform can be explained by examining the solubilities of the different anesthetics in water. The solubility of chloroform is 66.6 mM,[24] which is more than 4 times greater than those of enflurane and isoflurane. Therefore, under our experimental conditions, a higher concentration of chloroform would be present in the aqueous liposome solution. Subsequently, more chloroform would be available to partition into the bilayer and would likely account for chloroform appearing to behave differently than the other anesthetics.

The polarity (electric dipole moment) is correlated with the anesthetic position in the bilayer. Species with larger dipole moments tend to sequester near the headgroup region, whereas less polar anesthetics sequester closer to the tails.[26] The anesthetics with the largest dipole moments (~2 D), isoflurane and sevoflurane, have the lowest rate constants and extents of lipid mixing. Halothane and chloroform have intermediate dipole moments (~1 D).

The molecular volumes of the anesthetics can affect their abilities to localize and change locations within a bilayer. A molecule with a smaller volume could be more versatile in accommodating bilayers with the increased radii of curvature necessary for stalk formation and fusion.

It seems likely that the anesthetics that influence bilayer bending rigidity the most will have the greatest effect on lipid mixing (or fusion). These anesthetics appear to be chloroform and halothane. Interestingly, earlier work from our group showed some evidence in support of this hypothesis. Atomic force microscopy of halothane-containing unilamellar DOPC vesicles indicates that they do not collapse as readily on a mica surface as DOPC vesicles that are free of halothane.[27] This suggests

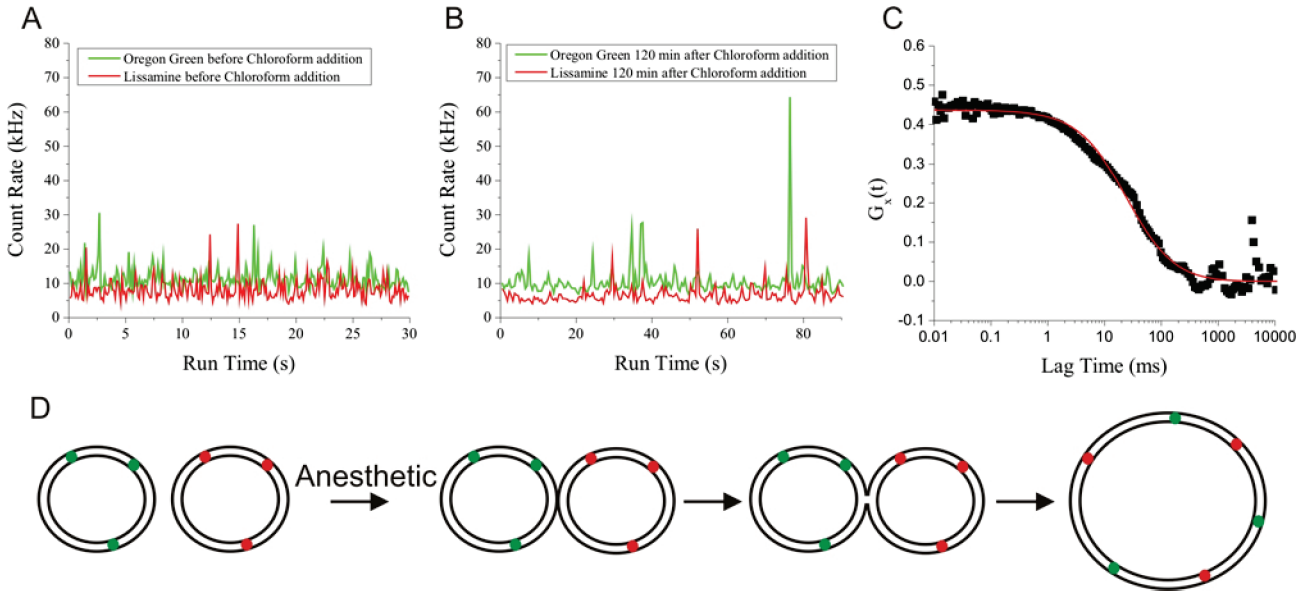

Figure 6. (A) Fluorescence count-rate trajectories for 400 nM lissamine-labeled (red) and 250 nM Oregon Green-labeled (green) DOPC (0.1 mM, lipid) vesicles prior to addition of halothane. (B) Fluorescence count-rate trajectories 60 min after addition of halothane (2% v/v). Note the increase in high-amplitude spikes in both channels, indicative of association. (C) Sample cross-correlation decay curve obtained using halothane as a fusion agent. The amplitude of the cross-correlation decay (G_x0) is proportional to the concentration of physically linked red- and green-labeled fluorescent species. (D) Schematic depiction of the vesicle association/fusion process. Samples were excited at 780 nm at a laser power of 30 mW.

that, with halothane incorporated, the vesicles might be under less curvature strain. Additionally, when halothane was added to a preformed supported planar bilayer, the lipid features formed resembled those of large vesicles, further suggesting that the thermodynamic-minimum structure for halothane-containing DOPC bilayers is curved.

As shown in Figure 5, a negligible change in monomer fluorescence was observed during the fusion/hemifusion of the two labeled vesicles. Therefore, we can assume that the large increases in monomer fluorescence that were observed in the FD assay can be attributed to lipid mixing of an unlabeled lipid vesicle with a fluorescently labeled lipid vesicle and not to bilayer swelling caused by the uptake of anesthetics into the lipid bilayer. However, it is possible that the less potent fusion agents (isoflurane, enflurane, and sevoflurane) do not actually induce complete fusion, but instead cause hemifusion. Hemifusion is a process in which the contacting lipid membrane leaflets mix, but the inner lipid membrane leaflets remain intact; therefore, no mixing of intervesicular contents occurs, as shown in the third panel of Figure 1.[4,6] We therefore chose to report our findings as lipid mixing and only speculate that the lower extent of lipid mixing could be associated with hemifusion.

Further, with the FD assay, it would be difficult to distinguish between stalk-formation- and pore-formation-induced lipid mixing. Because the data are best fit with a simple single rate constant, we suggest that this represents stalk formation as being rate-limiting. Otherwise, we would expect more complex kinetic plots. This would be similar to the first step in the stalk model proposed by Weinreb and Lentz.[17] Although they used a different lipid system, the rates are quite comparable, with the kinetics in the study about 10-fold slower for lipid mixing. This difference could be rationalized by the differences in lipid system and in the mechanism of induction.

Vesicle Association and Anesthetics. As stated above, the anesthetics that enhanced lipid mixing to the greatest degree were not the same as those that enhanced vesicle association. This suggests that a molecule's position in the bilayer influences its macroscopic effect. The rate constants obtained for the FCCS association assay, summarized in Table 1, were found to be

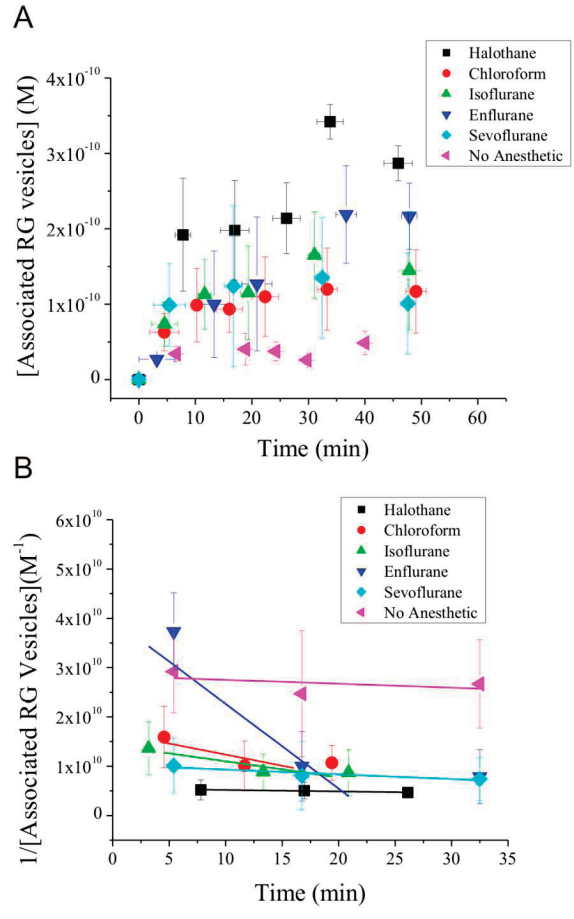

Figure 7. (A) Average kinetic curves for the association of lissamine (400 nM) and Oregon Green (250 nM) labeled DOPC (0.1 mM, lipid) vesicles induced by various anesthetics (2% v/v) obtained via fluorescence cross-correlation spectroscopy (FCCS). Concentrations of associated red and green vesicles were obtained from the amplitudes of cross-correlation decays. (B) Linearized data from A. The rate constants for the association of red and green vesicles were obtained from the slopes of the linearized data and are summarized in Table 1.

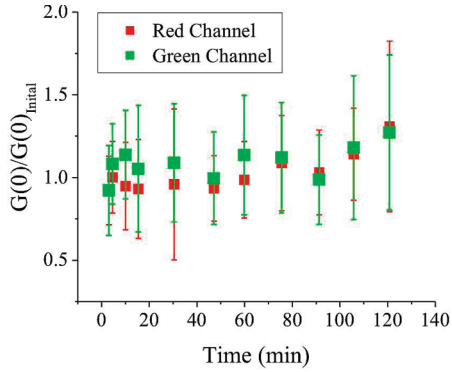

Figure 8. Plot of autocorrelation amplitudes [$G(0)$ values] of both red and green detection channels over time of a solution of lissamine (400 nM) and Oregon Green (250 nM) labeled DOPC (0.1 mM, lipid) vesicles after the addition of halothane (2% v/v). The constant amplitude observed is consistent with eq 18.

TABLE 2: Summary of Partition Coefficients at 37°C, Logarithms of Octanol/Water Partition Coefficients ($P_{octanol/water}$), and Water Solubilities for the General Anesthetics Halothane, Chloroform, Isoflurane, Enflurane, and Sevoflurane

anesthetic	solubility (mM)	partition coefficients (37 °C) oil/gas	water/gas	oil/water	log $P_{octanol/water}$
halothane	20.9[32]	197[24]	0.63[24]	313	2.70[33]
chloroform	66.6[24]	233[24]	3.8[24]	61	1.97[34]
isoflurane	15[24]	90.8[24]	0.54[24]	168	2.46[35]
enflurane	15[24]	96.5[24]	0.78[24]	124	2.19[35]
sevoflurane	6[36]	53.4[25]	0.36[25]	148	2.28[35]

rather different for each anesthetic. The rate constants for the association of labeled vesicles were found to follow the trend isoflurane > enflurane ≈ chloroform > sevoflurane ≈ halothane. The large differences in the vesicle association rate constants obtained for the general anesthetics indicate that some anesthetics decrease the energy barrier for vesicle association to a greater extent than other anesthetics. Clearly, this trend cannot be explained by partition coefficients and water solubilities alone, indicating that there must be additional properties that have an effect on the association rates, possibly by affecting the hydration of the bilayer headgroups.[9] Wen et al.[28] previously illustrated the ability of halothane and isoflurane to increase the dehydration of surfactants and trigger the formation of micelles. Therefore, it can be extrapolated that anesthetics such as halothane and isoflurane might also disturb the water of hydration surrounding biological membranes.[28]

It is of note that the vesicle association rate constants obtained using general anesthetics as fusion agents coincide well with rate constants previously reported for Ca^{2+}-induced fusion of DOPC/cardiolipin LUVs (2.1×10^8 M^{-1} min^{-1})[29] and Ca^{2+}-induced aggregation of phosphatidylserine (PS) LUVs [$(2.6-4.68) \times 10^9$ M^{-1} min^{-1}],[30] which further supports the claim that some general anesthetics can be utilized as novel fusion agents, as the partitioning of an anesthetic into the bilayer would perturb the contacting monolayers of the associated vesicles, therefore increasing the probability of lipid mixing and subsequent fusion pore fomation.[31] It is significant that, whereas the extent of lipid mixing varies with anesthetic (FD assay), the association events remain constant (TPE-FCCS assay). Thus, we can be confident that the measured lipid mixing is not due to sample variation.

Finally, it is clear from Figure 7A that the maximum concentrations of associated red and green vesicles were the same within the experimental error for all of the anesthetics examined. This suggests that, during the time scale of the experiments, eventually, all of the anesthetics induced the same number of association events between red and green vesicles.

Conclusions

We have demonstrated that some general anesthetics (i.e., halothane and chloroform) have a greater propensity to induce membrane fusion in model DOPC lipid membranes, which is related to their respective partition coefficients, aqueous solubilities, polarities, and sizes. Small molecules (anesthetics) that induce membrane fusion likely do so through the perturbation of the contacting monolayers of the associated vesicles, which results in a reduction of the energy barrier for stalk formation, likely through changes in the bending modulus of the bilayer. Our work further supports the theory that lipid rearrangement for stalk formation is the rate-limiting step in the membrane fusion mechanism of simple vesicles.

Acknowledgment. The authors are grateful to NSERC, CIPI, and AIF for funding this project.

Supporting Information Available: Descriptions of experiments designed to examine whether or not liposomes remain intact in a chloroform environment. This material is available free of charge via the Internet at http://pubs.acs.org.

References and Notes

(1) Markin, V. S.; Albanesi, J. P. *Biophys. J.* **2002**, *82*, 693–712.
(2) Horton, R.; Moran, L.; Ochs, R.; Rawn, D.; Scrimgeour, G. *Principles of Biochemistry*; Neil Patterson Publishers/Prentice-Hall, Inc.: Englewood Cliffs, NJ, 1992.
(3) Chernomordik, L.; Kozlov, M. M.; Zimmerberg, J. *J. Membr. Biol.* **1995**, *146*, 1–14.
(4) Langosch, D.; Hofmann, M.; Ungermann, C. *Cell. Mol. Life Sci.* **2007**, *64*, 850–864.
(5) Lee, J.; Lentz, B. *Proc. Natl. Acad. Sci. U.S.A.* **1998**, *95*, 9274–9279.
(6) Cummings, J. E.; Vanderlick, T. K. *Biochim. Biophys. Acta: Biomembr.* **2007**, *1768*, 1796–1804.
(7) Floyd, D. L.; Ragains, J. R.; Skehel, J. J.; Harrison, S. C.; van Oijen, A. M. *Proc. Natl. Acad. Sci. U.S.A.* **2008**, *105*, 15382–15387.
(8) Carnini, A.; Nguyen, T. T.; T., C. D. *Can. J. Chem.* **2007**, *85*, 513–519.
(9) Leonenko, Z. V.; Cramb, D. T. *Can. J. Chem.* **2004**, *82*, 1128–1138.
(10) Leonenko, Z. V.; Finot, E.; Cramb, D. *Biochim. Biophys. Acta: Biomembr.* **2006**, *1758*, 487–492.
(11) Swift, J. L.; Carnini, A.; Dahms, T. E. S.; Cramb, D. T. *J. Phys. Chem. B* **2004**, *108*, 11133–11138.
(12) Heinze, K.; Koltermann, A.; Schwille, P. *Proc. Natl. Acad. Sci. U.S.A.* **2000**, *97*, 10377–10382.
(13) Schwille, P.; Meyer-Almes, F.; Rigler, R. *Biophys. J.* **1997**, *72*, 1878–1886.
(14) Carnini, A.; Phillips, H.; Shamrakov, L.; Cramb, D. *Can. J. Chem.* **2004**, *82*, 1139–1149.
(15) Baber, J.; Ellena, J. F.; Cafiso, D. S. *Biochemistry* **1995**, *34*, 6533–6539.
(16) Norgrady, T. *Medicinal Chemistry: A Biochemical Approach*, 2nd ed.; Oxford University Press: New York, 1988.
(17) Weinreb, G.; Lentz, B. R. *Biophys. J.* **2007**, *92*, 4012–4029.
(18) Malinin, V. S.; Haque, M. E.; Lentz, B. R. *Biochemistry* **2001**, *40*, 8292–8299.
(19) Szoka, F.; Olson, F.; Heath, T.; Vail, W.; Mayhew, E.; Papahadjopoulos, D. *Biochim. Biophys. Acta* **1980**, *601*, 559–571.
(20) Swift, J. L.; Heuff, R.; Cramb, D. T. *Biophys. J.* **2006**, *90*, 1396–1410.
(21) Dougan, L.; Bates, S. P.; Hargreaves, R.; Fox, J. P.; Crain, J.; Finney, J. L.; Reat, V.; Soper, A. K. *J. Chem. Phys.* **2004**, *121*, 6456–6462.
(22) Dixit, S.; Crain, J.; Poon, W. C. K.; Finney, J. L.; Soper, A. K. *Nature* **2002**, *416*, 829–832.
(23) Okuda, C. *J. Biochem.* **1982**, *92*, 357–363.
(24) Roth, S. H.; Miller, K. W. *Molecular and Cellular Mechanisms of Anesthetics*; Plenum Medical Book Compay: New York, 1986.
(25) Wallin, R. F.; Regan, B. M.; Napoli, M. D.; Stern, I. J. *Anesthesia Analgesia* **1975**, *54*, 758–766.

(26) MacCallum, J. L.; Tieleman, D. P. Interactions between small molecules and lipid bilayers. In *Computational Modeling of Membrane Bilayers*; Elsevier Academic Press Inc: San Diego, CA, 2008; Vol. 60, pp 227−256.
(27) Shamrakov, L. G.; Cramb, D. T. *Can. J. Chem.* **2005**, *83*, 1190–1194.
(28) Wen, X. G.; Verrall, R. E.; Liu, G. J. *J. Phys. Chem. B* **1999**, *103*, 2620–2626.
(29) Lentz, B. R.; Lee, J. K. *Mol. Membr. Biol.* 1999*16*, 279–296.
(30) Wilschut, J.; Duzgunes, N.; Fraley, R.; Papahadjopoulos, D. *Biochemistry* **1980**, *19*, 6011–6021.
(31) Lee, J.; Lentz, B. R. *Biochemistry* **1997**, *36*, 6251–6259.
(32) Ogata, Y.; Sugihara, K.; Sakka, T.; Iwasaki, M. *J. Fluorine Chem.* **1992**, *57*, 285–292.
(33) Urban, B. W.; Bleckwenn, M.; Barann, M. *Pharmacol. Therapeut.* **2006**, *111*, 729–770.
(34) Hansch, C.; Vittoria, A.; Silipo, C.; Jow, P. Y. C. *J. Med. Chem.* **1975**, *18*, 546–548.
(35) Franks, N. P.; Lieb, W. R. *Anesthesiology* **1996**, *84*, 716–720.
(36) Sekiya, A.; Misaki, S. *J. Fluorine Chem.* **2000**, *101*, 215–221.
(37) Zubrzycki, I. Z.; Xu, Y.; Tang, P. *Anesthesiology* **2000**, *93*, A121.
(38) Liu, R. Y.; Meng, Q. C.; Xi, J.; Yang, J. S.; Ha, C. E.; Bhagavan, N. V.; Eckenhoff, R. G. *Biochem. J.* **2004**, *380*, 147–152.
(39) Wormald, C. J.; Johnson, P. W. *J. Chem. Soc., Faraday Trans.* **1998**, *94*, 1267–1270.
(40) Braswell, L. M.; Kitz, R. J. *J. Neurochem.* **1977**, *29*, 665–671.
(41) Liu, R. Y.; Eckenhoff, R. G. *Anesthesiology* **2005**, *102*, 799–805.

JP901089K